

The Monothiol Single-Domain Glutaredoxin Is Conserved in the Highly Reduced Mitochondria of *Giardia intestinalis*^{†‡}

Petr Rada,¹ Ondřej Šmíd,¹ Robert Sutak,¹† Pavel Doležal,¹ Jan Pyrih,¹ Vojtěch Žárský,¹
Jean-Jacques Montagne,² Ivan Hrdý,¹ Jean-Michel Camadro,² and Jan Tachezy^{1*}

Department of Parasitology, Faculty of Science, Charles University in Prague, Viničná 7, Prague 2, 128 44, Czech Republic,¹ and
Institut Jacques Monod, Bâtiment Buffon, 15 rue Hélène Brion, 75205 Paris Cedex 13, France²

Received 22 June 2009/Accepted 6 August 2009

The highly reduced mitochondria (mitosomes) of *Giardia intestinalis* are recently discovered organelles for which, it was suggested, iron-sulfur cluster assembly was their only conserved function. However, only an incomplete set of the components required for FeS cluster biogenesis was localized to the mitosomes. Via proteomic analysis of a mitosome-rich cellular fraction together with immunofluorescence microscopy, we identified a novel mitochondrial protein homologous to monothiol glutaredoxins containing a CGFS motif at the active site. Sequence analysis revealed the presence of long nonconserved N-terminal extension of 77 amino acids, which was absent in the mature protein. Expression of the complete and N-terminally truncated forms of the glutaredoxin indicated that the extension is involved in glutaredoxin import into mitosomes. However, the mechanism of preprotein processing is unclear, as the mitochondrial processing peptidase is unable to cleave this type of extension. The recombinant mature protein was shown to form a homodimeric structure, which binds a labile FeS cluster. The cluster is stabilized by glutathione and dithiothreitol. Phylogenetic analysis showed that giardial glutaredoxin is related to the mitochondrial monothiol glutaredoxins involved in FeS cluster assembly. The identification of a mitochondrial-type monothiol glutaredoxin in the mitosomes of *G. intestinalis* thus completes the mitochondrial FeS cluster biosynthetic pathway and provides further evidence for the mitochondrial origin of these organelles.

Giardia intestinalis is a parasitic protist that was considered amitochondrial until recently (7). Although typical ATP-producing mitochondria are not present, related organelles, named mitosomes, were discovered in this organism (29). Mitosomes and mitochondria have a number of similarities; most notably, both are surrounded by a double membrane (29), they have a common mode of protein import and maturation (6, 24), and both harbor key components of the FeS cluster assembly machinery (29). These similarities indicate that mitosomes are highly reduced forms of mitochondria (7, 30), even though alternative evolutionary scenarios are still being discussed (17).

FeS clusters are cofactors of a number of FeS proteins involved mainly in electron transport, energetic metabolism, synthetic pathways, and biological sensing (12). Most importantly, the FeS protein Rli1 is indispensable for rRNA processing and ribosome biogenesis (15, 31). Consequently, the biogenesis of FeS clusters is an essential process for all cells from bacteria to human cells (15). In most nonplant eukaryotes, the crucial part of this biosynthetic pathway occurs in the mitochondrion or mitochondrion-related organelles (14, 24, 28). Studies of *Saccharomyces cerevisiae* mitochondria showed that the FeS cluster

assembly is centered on IscU, a metallochaperone that serves as a scaffold for a new FeS cluster. The cysteine desulfurase IscS (in *S. cerevisiae* named Nfs1) forms a heterodimer with Isd11. This heterodimer catalyzes the mobilization of sulfur for the FeS cluster. The delivery of iron is most likely regulated by frataxin (1). Reducing equivalents, which are required during FeS cluster biogenesis, are provided by a short electron transport chain, including the mitochondrial [2Fe2S] ferredoxin and ferredoxin:NADH reductase. Finally, a transient FeS cluster is transferred from IscU (Isu1/2) to apoproteins by the action of the Hsp70 (Ssq1) and Hsp40 (Jac1) chaperones and the proteins IscA (Isa1/2) and Iba57 (15). This last step also requires a monothiol class glutaredoxin (Grx5) with a characteristic CGFS active site motif (20). This class of glutaredoxins catalyzes the reduction of disulfide bonds in proteins converting glutathione (GSH) to GSH disulfide. It has been recently demonstrated that dimeric monothiol glutaredoxins can coordinate a [2Fe2S] cluster via the cysteine residue of the active site of each monomer and the cysteines of two GSH molecules (20). Although the exact role of Grx5 remains to be elucidated, it was hypothesized that, in the final step of iron sulfur cluster biogenesis, the FeS cluster that is transiently formed on an IscU scaffold protein is transferred to a Grx5 dimer in a GSH-dependent manner and is subsequently passed on to the target apoproteins (20).

The ability of *Giardia* mitosomes to assemble FeS clusters on apoferredoxin has been demonstrated (29), indicating that all necessary components of the FeS cluster assembly machinery are present in these organelles. However, only three components known from *S. cerevisiae* mitochondria have been shown to be localized to mitosomes so far (IscS, IscU, and

* Corresponding author. Mailing address: Charles University in Prague, Faculty of Science, Department of Parasitology, Viničná 7, 128 44 Prague, Czech Republic. Phone: 420-221-951-811. Fax: 420-224-919-704. E-mail: tachezy@natur.cuni.cz.

† Supplemental material for this article may be found at <http://ec.asm.org/>.

‡ Present address: Institut Jacques Monod, Bâtiment Buffon, 15 rue Hélène Brion, 75205 Paris Cedex 13, France.

[‡] Published ahead of print on 28 August 2009.

[2Fe2S] ferredoxin), while some others, including Isd11, frataxin, and GSH, were reported to be absent in *Giardia* (4, 5, 21). In this study we identified monothiol glutaredoxin in a mitosome-enriched fraction of *G. intestinalis* (Gigrx) using a proteomic approach. The mitosomal localization of Gigrx was confirmed by expression of the tagged protein in *Giardia* cells. The protein contains an unusually long N-terminal extension, which is involved in targeting the protein to the organelle, while the C-terminal part contains conserved residues required for the coordination of an FeS cluster. Phylogenetic analysis showed the close relationship between Gigrx and its mitochondrial homologues, which is consistent with the proposed mitochondrial origin of the iron-sulfur cluster assembly machinery in *G. intestinalis*.

MATERIALS AND METHODS

Reagents. Acetonitrile, α -cyano-4-hydroxycinnamic acid, dithiothreitol (DTT), *N*- α -tosyl-L-lysine chloromethyl ketone, leupeptin, polyvinylidene difluoride membranes, protein A-Sepharose, reduced and oxidized GSH, sucrose, Tris, trifluoroacetic acid, trypsin, CaCl_2 , KCl, and NH_4HCO_3 were purchased from Sigma-Aldrich.

Cell cultivation. The *G. intestinalis* strain WB (American Type Culture Collection; ATCC 30957) was grown in TYI-S-33 medium supplemented with 10% heat-inactivated bovine serum (PAA Laboratories, GmbH, Austria), 0.1% bovine bile, and antibiotics (13).

Preparation of mitosome-rich fractions. *Giardia* trophozoites were harvested, washed twice in ST buffer (250 mM sucrose, 0.5 mM KCl, 10 mM Tris [pH 7.2]), and suspended in ST buffer with 50 $\mu\text{g}/\text{ml}$ *N*- α -tosyl-L-lysine chloromethyl ketone and 10 $\mu\text{g}/\text{ml}$ leupeptin. The cells were disrupted by sonication and centrifuged at $680 \times g$ for 10 min and at $2,760 \times g$ for 20 min to remove unbroken cells, nuclei, and cytoskeletal residues. The supernatant was centrifuged at $50,000 \times g$ for 30 min. The high-speed supernatant was used for preparation of the cytosolic fraction by centrifugation at $250,000 \times g$ for 30 min. The high-speed pellet was resuspended in 0.5 ml of ST buffer and layered onto a discontinuous sucrose gradient consisting of 1 ml each of 25%, 30%, 35%, 40%, 45%, 50%, 55%, and 60% sucrose in 25 mM Tris-HCl, pH 7.2. The gradient was centrifuged for 22 h in a Beckman SW40 rotor at $120,000 \times g$ and 4°C . Fractions (0.5 ml each) were collected and analyzed by immunoblotting using polyclonal rabbit anti-GiiscU antibody (29). The concentrations of sucrose in the collected fractions were determined by refractometry.

2D PAGE. The mitosome-rich fraction was washed with ST buffer, solubilized in 7 M urea, 2 M thiourea, 4% CHAPS {3-[(3-cholamidopropyl)-dimethylammonio]-1-propanesulfonate}, 0.5% Bio-Lyte ampholyte (Bio-Rad), 100 mM DTT, bromophenol blue, and 40 mM Tris, pH 8.8, and subjected to isoelectric focusing on 17-cm, pH 3 to 10 and pH 4 to 7 immobilized pH gradient strips (Bio-Rad). After the focusing, the gel strips were equilibrated twice for 15 min each with 6 M urea, 20% glycerol, 50 mM Tris (pH 8.2), 2% sodium dodecyl sulfate (SDS), 65 mM DTT, and bromophenol blue. The second dimension was run on 13.5% SDS-polyacrylamide gel electrophoresis (PAGE) gels, and the separated proteins were stained with Coomassie brilliant blue G250. Gel images were analyzed using PDQuest two-dimensional (2D) analysis software (Bio-Rad).

Trypsin digestion and mass spectrometry. Protein spots were manually excised from the 2D gels, washed twice with 25 mM NH_4HCO_3 , dehydrated in acetonitrile, dried, and subjected to in-gel digestion by rehydration with 10 μl trypsin, 25 mM NH_4HCO_3 , and 5 mM CaCl_2 . Digestion was performed at 37°C overnight. Tryptic peptides were extracted by subsequent washing with 50% acetonitrile–0.1% trifluoroacetic acid and 100% acetonitrile–0.1% trifluoroacetic acid. The washes were pooled, desalted with a C18 ZipTip (Millipore), and analyzed in a Voyager-DE PRO matrix-assisted laser desorption/ionization–time of flight mass spectrometer (Applied Biosystems). A saturated solution of α -cyano-4-hydroxycinnamic acid in 50% acetonitrile and 0.1% trifluoroacetic acid was used as the matrix. The spectra were analyzed using an in-house Mascot search engine (Matrix Science, London, United Kingdom) with a local implementation of GiardiaDB v1.1 proteins and translated coding sequences.

Sequence analyses. Putative cleavage sites for mitochondrial processing peptidase were predicted with PsortII (<http://psort.ims.u-tokyo.ac.jp/>) and MitoProt II (<http://ihg2.helmholtz-muenchen.de/ihg/mitoprot.html>). The Gigrx sequence was aligned to the glutaredoxin sequences of *S. cerevisiae* (NCBI accession no.

Q02784), *Caulobacter* sp. strain K31 (NCBI accession no. YP_001685091), and *Synechocystis* sp. strain PCC 6803 (NCBI accession no. NP_440398) using ClustalW (28) and manually edited with BioEdit (10). For phylogenetic reconstruction, glutaredoxin-related sequences were identified by BLAST searches (<http://blast.ncbi.nlm.nih.gov/Blast.cgi>), aligned using ClustalX, and manually edited with BioEdit (10). The Bayesian method was used for detailed analysis of glutaredoxin clades. Bayesian searches of tree space were performed with MrBayes (23) using the JTT amino acid substitution matrix with one invariable Γ rate category and four variable Γ rate categories. Four Monte Carlo Markov chains, each with 100,000 generations, were performed, with trees sampled every 100 generations. For compilation of Bayesian consensus topologies, a “burn-in” of 600 trees was used.

Selectable transformation of *G. intestinalis* and immunofluorescence analysis. A gene coding for the complete *G. intestinalis* glutaredoxin (*gigrx*^{1–202}; GiardiaDB identification number GL50803_2013; <http://www.giardiadb.org/giardiadb/>) and its truncated form coding for amino acids 65 to 202 (*gigrx*^{65–202}; numbers according to Fig. 3) were amplified by PCR using the forward primers GigrxF1 (5'-CATGCATATGGACCAATAAACGGG-3') and GigrxF2 (5'-CATGCATATGCCAGTGTGTCTCCCTG-3') and reverse primer GigrxR (5'-CATGGGATCCGTCTGGTAGGCCACACACCTT-3'). cDNA was used as template, which was prepared as previously described (6). PCR products were inserted into the plasmid pONDRA-HA (6). Cells were transformed and selected as described in reference 25. *G. intestinalis* cells expressing recombinant proteins fused with a hemagglutinin (HA) tag at the C terminus were fixed and stained for immunofluorescence microscopy with mouse monoclonal anti-HA antibody (6). In double-labeling experiments, GiiscU was detected as a mitosomal marker protein using rabbit polyclonal anti-GiiscU antibody (29). Alexa Fluor-488 (green)-donkey anti-mouse antibody and Alexa Fluor-594 (red)-donkey anti-rabbit antibody (Invitrogen) were used as secondary antibodies (6). The slides were examined with an Olympus IX81 microscope equipped with an MT20 illumination system. The images were processed using ImageJ 1.41e software (NIH).

Protein expression and purification. *gigrx*^{1–202} and *gigrx*^{99–202} were inserted into the pET42b and pQE30 (Qiagen) vectors, respectively, for expression of the proteins with a C-terminal (pET42) or N-terminal (pQE) hexahistidine tag in *Escherichia coli*. The expression and purification of *gigrx*^{1–202} were performed under denaturing conditions using Ni-nitrilotriacetic acid affinity chromatography according to the manufacturer's protocol (Qiagen, GmbH, Hilden, Germany). The expression of *gigrx*^{99–202} was induced by 0.5 mM isopropyl- β -D-thiogalactopyranoside, and the bacteria were grown at 20°C overnight using Luria-Bertani medium supplemented with 0.5 mM ferric ammonium citrate and GSH. *gigrx*^{99–202} was purified by Ni-nitrilotriacetic acid affinity chromatography under native conditions (Qiagen, GmbH, Hilden, Germany). The active mitosomal processing peptidase (GPP) was prepared and cleavage of *gigrx*^{1–202} was tested as described in reference 24.

Immunoblot analysis. Samples of cell fractions were separated using 13% SDS-PAGE, and, after transfer to a nitrocellulose membrane, giardial glutaredoxin was detected using polyclonal rat antibody, which was raised against recombinant *gigrx*^{99–202} by Moravian Biotechnology Ltd. (Czech Republic). The expression and processing of HA-tagged Gigrx in *Giardia* were followed using mouse monoclonal anti-HA antibody (Exbio Prague a.s., Czech Republic).

Immunoprecipitation and N-terminal amino acid sequencing. C-terminally HA-tagged Gigrx was immunoprecipitated from the mitosome-rich fraction of *G. intestinalis* expressing *gigrx*^{1–202} using mouse monoclonal anti-HA antibody and protein A-Sepharose as described in reference 19. Immunoprecipitated Gigrx was separated by SDS-PAGE (13% gel), transferred onto a polyvinylidene difluoride membrane, and subjected to N-terminal protein sequencing by Edman degradation (Institute of Organic Chemistry and Biochemistry, Academy of Sciences of the Czech Republic).

Analytical methods. UV-visual spectra of freshly purified *gigrx*^{599–203} were monitored at room temperature between 260 and 700 nm using a Shimadzu UV-1601 spectrophotometer.

RESULTS

Isolation of the mitosome-rich fraction and identification of glutaredoxin by mass spectrometry. An enrichment of *Giardia intestinalis* mitosomes in subcellular fractions was achieved by centrifugation of the high-speed sediment of sonicated cells in a discontinuous sucrose gradient (25% to 60% [vol/wt] sucrose) (Fig. 1). Experiments using Percoll or metrizamide gra-

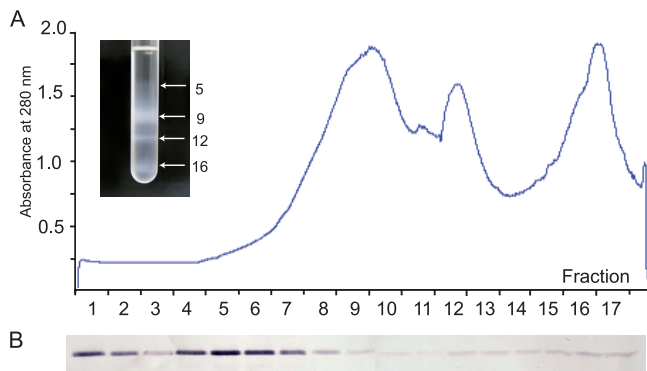


FIG. 1. (A) Purification of the mitosome-rich fraction of *Giardia*. Separation of a high-speed pellet of sonicated cells on a discontinuous sucrose gradient (25 to 60%) is shown in the inset. Numbers correspond to collected fractions. The curve corresponds to protein amounts in the fractions. (B) Western blot analysis of collected fractions using rabbit polyclonal anti-GiiscU antibody.

dients did not lead to mitosome separation in our experiments (data not shown). Seventeen fractions were collected, and the separation of mitosomes was followed by immunoblot analyses of each fraction using IscU as a mitosomal marker protein (Fig. 1). Fractions 5 and 6 (44 to 49% sucrose) with the highest signal for IscU were pooled and further used for 2D gel separations (Fig. 2). Twenty-five of the most abundant spots were selected for mass spectrometry, among which four known mitosomal proteins (GiiscS, GiiscU, Hsp70, and Cpn60) were identified (Fig. 2; see Table S1 in the supplemental material for the complete list of identified proteins). Tryptic peptide sequences obtained from two protein spots on 2D gels corresponded to a glutaredoxin-related protein (Gigrx) annotated at GiardiaDB (www.giardiadb.org/giardiadb/; identification no. GL50803_2013). The first protein displayed an approximate

molecular size of 14.6 kDa, with pI 6, and the second protein was 14.9 kDa, with pI 5.3. All tryptic fragments derived from both proteins were localized to the C-terminal part of Gigrx, whose predicted molecular size was 22.1 kDa and pI value was 7.7 (Fig. 3). The first peptide determined by mass spectrometry started at Thr 81.

Gigrx contains an N-terminal extension which is involved in targeting the protein to mitosomes. A comparison of the predicted amino acid sequences of Gigrx with its mitochondrial and bacterial orthologs revealed an N-terminal extension of about 98 amino acids preceding the conserved Grx domains (Fig. 3). Such an extension may serve as the targeting presequence, which is required for the translocation of a protein to mitosomes and which is cleaved off by a mitosomal processing peptidase (24). However, all known mitosomal targeting presequences are rather short (24). Indeed, two programs designed for the prediction of mitochondrial N-terminal presequences, PsortII and MitoProt II, predicted the first 19 to 23 amino acids of the extension as putative mitochondrial targeting presequences and suggested either SRG/LI (PsortII) or TRY/AS (MitoProt II) motifs as putative cleavage sites for the mitochondrial processing peptidase. However, the calculated size of Gigrx, processed according to predicted cleavage sizes, was about 20 kDa, which did not correspond to the form of Gigrx observed on 2D gels. Thus, we raised a rat anti-Gigrx polyclonal antibody to verify which form(s) of Gigrx is present in mitosomes. Immunoblot analysis confirmed that Gigrx is present as a 14.5-kDa protein. Neither the protein corresponding to the molecular sizes of the predicted processed forms (about 20 kDa) nor the full-length preprotein (22 kDa) was observed (Fig. 4).

We next prepared a construct for the expression of full-length Gigrx (Gigrx^{1–202}) with a C-terminal HA tag in *Giardia*. In transformed cells overexpressing Gigrx^{1–202} we observed two forms of Gigrx corresponding to the preprotein (upper

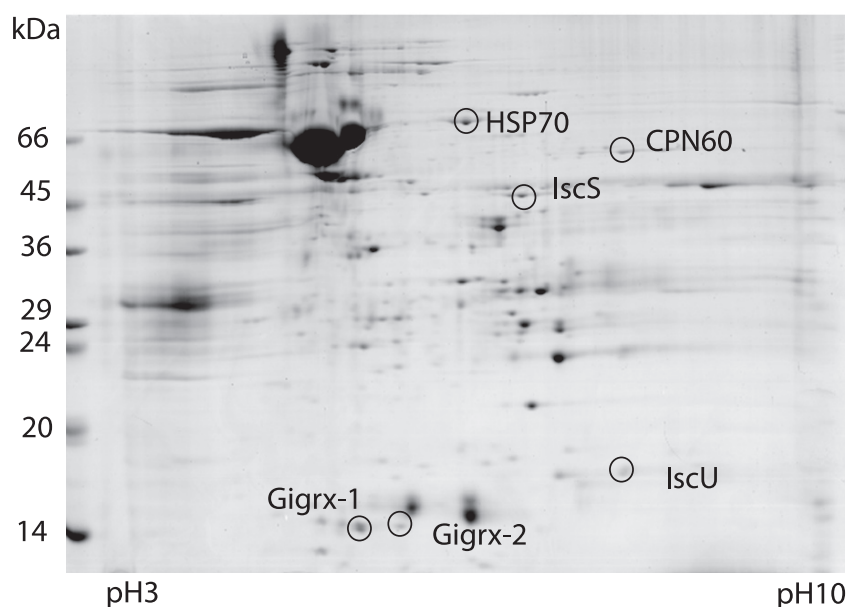


FIG. 2. 2D electrophoresis of the mitosome-rich fraction. A representative pH 3 to 10 gradient 2D gel is shown, with four mitosomal marker proteins (HSP70, CPN60, IscS, and IscU) and two spots of identified glutaredoxins.

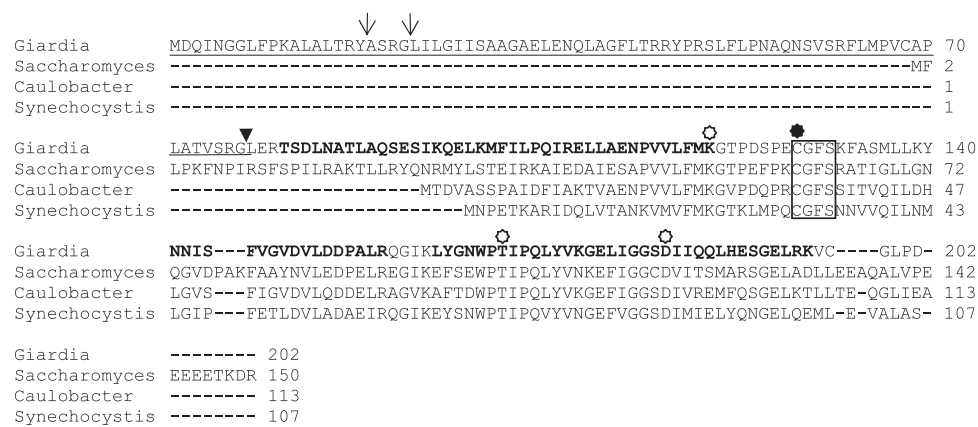


FIG. 3. Alignment of *Giardia intestinalis* glutaredoxin (Gigrx), the mitochondrial monothiol Grx5 of *S. cerevisiae* (NCBI accession no. Q02784), and bacterial monothiol Grx of *Caulobacter* sp. strain K31 (NCBI accession no. YP_001685091) and *Synechocystis* sp. strain PCC 6803 (NCBI accession no. NP_440398). The N-terminal targeting presequence of Gigrx is underlined. PSORT II (SRG/LI)- and MitoProt (TRY/AS)-predicted cleavage sites for mitochondrial processing peptidase are marked with arrows. The arrowhead indicates the cleavage site determined by N-terminal amino acid sequencing of Gigrx immunoprecipitated from mitosomes. The conserved CGFS motif is boxed. The amino acid residues involved in GSH binding are indicated by open asterisks. The cysteine residue that coordinates the FeS cluster is indicated by a solid asterisk.

band) and mature Gigrx (lower band) (Fig. 5). To identify the preprotein cleavage site, mature tagged Gigrx was immunoprecipitated from the mitosomal cellular fraction. The N-terminal sequencing of the mature protein by Edman degradation revealed the cleavage site to be between glycine 77 and leucine 78 (SRG/LE motif) (Fig. 3).

To test this protein cleavage experimentally, *E. coli*-produced Gigrx¹⁻²⁰², which was fused with a hexahistidine tag at the C terminus, was incubated with recombinant *S. cerevisiae* mitochondrial and giardial mitosomal processing peptidases (24). However, no cleavage of the Gigrx preprotein was observed at either of the in silico-predicted sites or the cleavage site determined for the immunoprecipitated mature protein (see Fig. S1 in the supplemental material).

Transcription of the gene coding for Gigrx, including the N-terminal extension, was confirmed by means of reverse tran-

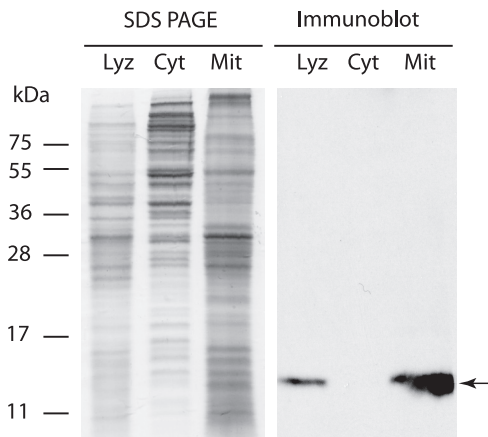


FIG. 4. Detection of Gigrx in *G. intestinalis* cellular fractions. Protein samples of cell lysate (Lyz), the cytosolic fraction (Cyt), and the mitosome-rich fraction (Mit) were separated by 13% SDS-PAGE and stained with Coomassie brilliant blue or transferred onto a nitrocellulose membrane for immunodetection using rat polyclonal anti-Gigrx antibody. The arrow indicates Gigrx in the mitosome-rich fraction.

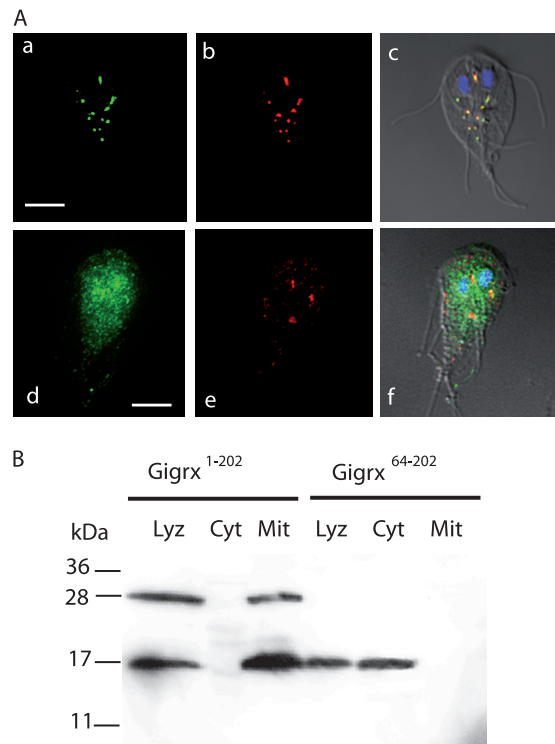


FIG. 5. Cellular localization of *G. intestinalis* glutaredoxin. (A) Transformed *G. intestinalis* cells expressed full-length Gigrx¹⁻²⁰² (a to c) or its N-terminally truncated form Gigrx⁶⁵⁻²⁰² (d to f). Recombinant proteins, fused at the C terminus with a HA tag, were stained for immunofluorescence microscopy using mouse anti-HA antibody (green). The mitochondrial marker protein GiisU was detected with the polyclonal rabbit anti-GiisU antibody (red). The merged images (c and f) showing Gigrx, GiisU, and the nuclei stained with DAPI (4',6-diamidino-2-phenylindole; blue) were produced by differential interference contrast. Scale bars, 4 μ m. (B) Immunoblot analysis of cellular fractions isolated from transformed *G. intestinalis* cells expressing Gigrx¹⁻²⁰² or Gigrx⁶⁵⁻²⁰². Monoclonal antibody against the HA tag was used to detect recombinant Gigrx. Lyz, Cyt, and Mit are as defined for Fig. 4.

scription-PCR (data not shown). Two putative start sites at positions 1 and 65 are present in the N-terminal extension (Fig. 3). Interestingly, when we used a truncated sequence of Gigrx in which 64 N-terminal amino acids were removed (Gigrx^{65–202}), PsortII recognized the same cleavage site between glycine 77 and leucine 78, which was experimentally determined for the mature Gigrx. Thus, we investigated whether the complete N-terminal extension is required for targeting this protein or whether the shorter Gigrx version can mediate this function. Two constructs for the expression of Gigrx^{1–202} and Gigrx^{65–202} were prepared, and their cellular localizations were compared by immunofluorescence microscopy (Fig. 5). Gigrx^{1–202} clearly colocalized with the mitochondrial marker protein GiiscU. The label corresponded with organelles organized into rodlike structures between two nuclei and with separate tiny organelles scattered mainly within the posterior part of the body, which is a typical distribution of *Giardia* mitochondria (27). In contrast, no mitochondrial localization of Gigrx^{65–202} was observed. These findings were corroborated by immunoblot analysis of cellular fractions. While Gigrx^{1–202} in the form of the preprotein as well as the mature protein was associated with the mitochondria-rich fraction, Gigrx^{65–202} was exclusively detected in the cytosol (Fig. 5).

Taken together, these results showed that the Gigrx preprotein contains a long N-terminal targeting presequence of 77 amino acids, which is required for protein translocation into the organelle and which is absent in the mature Gigrx.

Domain structure and phylogeny of *G. intestinalis* glutaredoxin. Sequence analysis of the C-terminal part of Gigrx (100 to 202 amino acids) revealed the presence of a single glutaredoxin domain with a monothiol consensus CGFS motif at the active site (Fig. 3). This structure is typical for mitochondrial glutaredoxins such as Grx5 in *S. cerevisiae* and those found in alphaproteobacteria, which exhibited a high sequence identity to Gigrx (52.4% and 44.2% for *Caulobacter* sp. strain K31 and *S. cerevisiae* Grx5, respectively). The affinity of Gigrx to mitochondrial orthologs is apparent from the phylogenetic analysis based on the Bayesian method, in which Grx5-type glutaredoxins formed a distinct mitochondrial cluster (Fig. 6). Two other major clusters of glutaredoxins, which are present in various cell compartments of eukaryotes, were also resolved: dithiol glutaredoxins, which typically possess a CPYC consensus motif, and multidomain monothiol glutaredoxins, which contain an N-terminal thioredoxinlike domain and multiple C-terminal monothiol Grx domains (2, 16). This analysis suggests a mitochondrial origin of Gigrx, which likely shares ancestry with other mitochondrial proteins involved in iron-sulfur cluster biosynthesis in *G. intestinalis* (26).

Homodimeric Gigrx coordinates the FeS cluster. The predicted Gigrx sequence contains all the residues crucial for the binding of GSH and coordination of the FeS cluster: Lys 120, Thr 168, and Asp 183, corresponding to Lys 23, Thr 71, and Asp 86 of *Synechocystis* monothiol glutaredoxin SyGrx3p (20). Therefore, we tested the possible formation of an FeS cluster on Gigrx. The C-terminal part of Gigrx with a His tag at the N terminus was expressed in *E. coli* and affinity purified to homogeneity. The isolated Gigrx was brown, as noticed previously for other FeS cluster-binding glutaredoxins (20). Optimal recovery of the colored protein was obtained when induced bacteria were grown overnight at 20°C in Luria-Bertani me-

dium supplemented with ferric ammonium citrate and GSH. The UV-visible absorption spectra of recombinant Gigrx displayed a prominent peak at 410 nm and shoulders at 320, 510, and 590 nm (Fig. 7). This spectral profile corresponded to [2Fe2S] glutaredoxins of *Synechocystis* and other organisms (20). However, the absorption decreased in time, indicating instability of the FeS cluster. The cluster stability increased with addition of GSH and DTT, while GSH disulfide had little effect. The addition of EDTA led to the loss of the absorbance at 320 to 590 nm.

When freshly isolated Gigrx was analyzed by gel filtration under native conditions, two protein subpopulations were isolated, with molecular masses of about 17.8 and 37.6 kDa. The absorbance at 410 nm was associated only with the 37.6-kDa protein. SDS-PAGE analysis of both denatured subpopulations showed a single protein with the lower molecular mass (Fig. 8). These results indicate that the FeS cluster is coordinated by a homodimeric Gigrx structure.

DISCUSSION

Proteomic analysis of the mitochondria-enriched cellular fraction together with localization studies by immunofluorescence microscopy of *Giardia intestinalis* revealed the presence of a CGFS-type glutaredoxin (Gigrx) in the mitochondria of this parasitic protist. Eukaryotes contain a series of glutaredoxins across various cellular compartments, where they carry out site-specific redox reactions. According to the consensus motif found in the active site of the glutaredoxin domain and the type of reaction they mediate, the proteins are classified into dithiol and monothiol groups. Dithiols use two cysteinyl groups with the consensus sequence CPYC in the reduction of protein disulfides, while monothiols (CGFS) rely purely on the N-terminal cysteinyl residue of the motif. Whereas the former exist as single-domain proteins, the latter can also build up multidomain proteins with up to three monothiol glutaredoxin domains and a thioredoxin domain. For example, in *Arabidopsis thaliana* approximately 50 genes encode glutaredoxinlike proteins with specific functions in various cellular compartments. In contrast, Gigrx is the only glutaredoxinlike protein which is present in the genome of *Giardia intestinalis*. This glutaredoxin type (also named Grx5) is specifically present in mitochondria. Several lines of evidence suggested that Grx5 is involved in the formation of the FeS clusters required for the maturation of FeS proteins. The genomic knockout of Grx5 in *S. cerevisiae* led to the impaired function of enzymes containing an FeS cluster in their catalytic sites (22). Another phenotype of Grx5-deficient mitochondria was an increase in iron load on the FeS scaffold protein IscU (Isu1 in *S. cerevisiae*), suggesting that Grx5 is required for inserting the prebuilt FeS cluster into the target apoproteins (18). More recently, it was suggested that CGFS-type Grx is an alternative scaffold to accommodate transient [2Fe2S] clusters in chloroplasts (3). Although its precise biochemical role is not clear, it seems that Grx5 is involved in the later steps of FeS cluster biogenesis. The presence of Grx5 in the highly reduced proteome of the *G. intestinalis* mitochondria underlines its importance for FeS cluster assembly, the only known function of these organelles. Unlike mitochondria, mitochondria have no known FeS proteins except

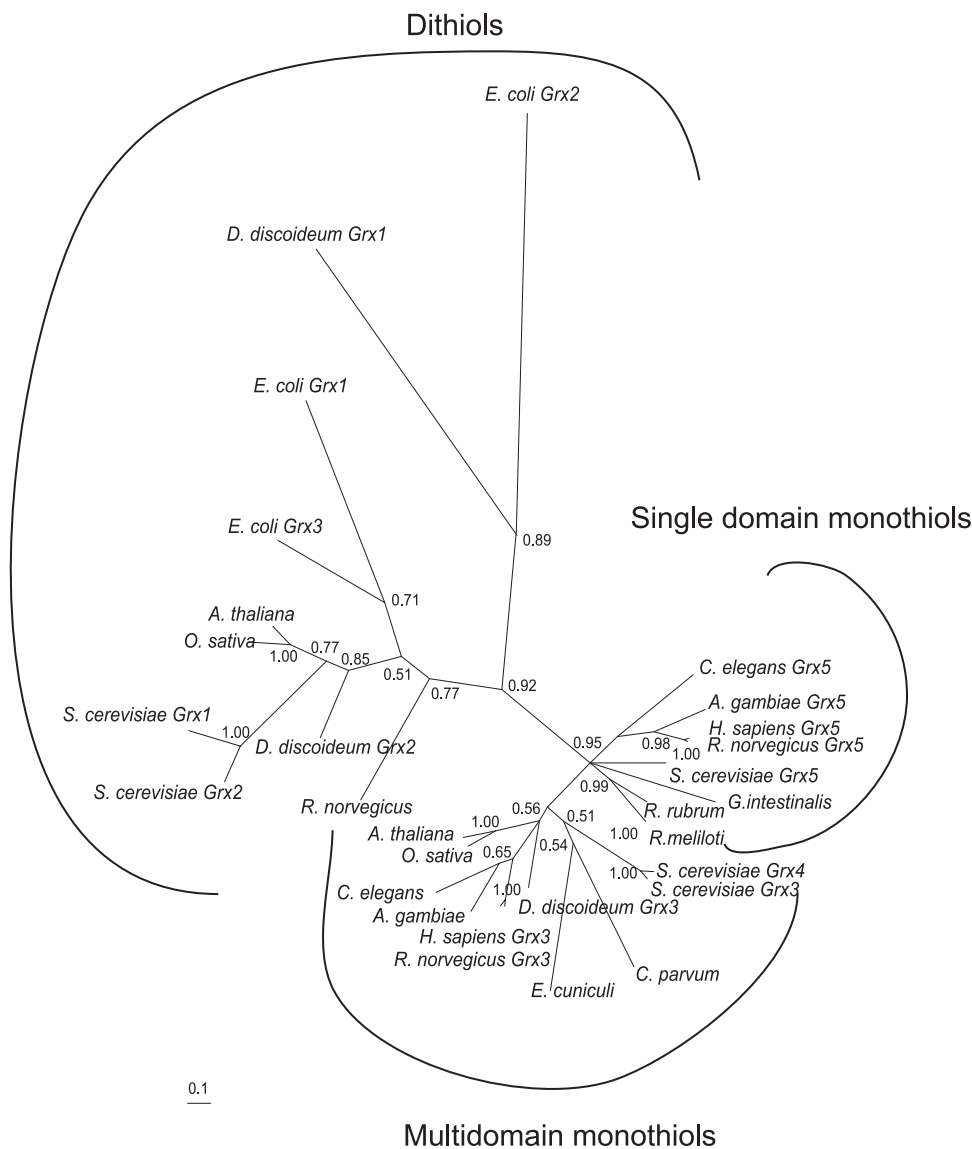


FIG. 6. Protein maximum-likelihood phylogenetic tree of selected glutaredoxin sequences. The tree was obtained using the program MrBayes (23) under the JTT substitution matrix with amino acid frequencies estimated from the data set. Numbers at the individual nodes represent MrBayes credibility values.

for those which are members of the FeS cluster assembly machinery (IscU, IscA, and [2Fe2S] ferredoxin). Thus, Gigrx is likely required either for the functioning of the FeS cluster assembly machinery itself or for the synthesis of FeS clusters or compounds, which can then be exported from the organelle to the cytosol for the maturation of extramitochondrial FeS proteins (14).

Our experiments showed that the Gigrx homodimer coordinates FeS clusters with spectral properties corresponding to those of [2Fe2S] clusters as in other monothiol CGFS-type glutaredoxins (20). The cysteine of the CGFS motif has been shown to be essential for the assembly of an FeS cluster and also for dimerization of the protein (20). Mutation of this cysteine in SyGrx3p of *Synechocystis* led to the formation of a monomeric colorless protein (20). The [2Fe2S] cluster bridging two Grx monomers is anchored by four cysteinyl residues. Two

cysteinyl residues are provided by the cysteines of the CGFS motif of each monomer, while the free thiol groups of GSH donate the other two cysteine residues. GSH is also required for the ligation of FeS clusters in other FeS cluster binding glutaredoxins, such as the CGYC-type dithiol Grx-C1 in *Populus tremula* (8). Interestingly, an earlier study reported the absence of GSH in *G. intestinalis* (4). Although high-pressure liquid chromatography analysis of the whole-cell lysate led to the proposal that cysteine is the major low-molecular-weight thiol in this organism, our search in the *Giardia* genome revealed the presence of genes coding for two key enzymes required for GSH synthesis, glutamate-cysteine ligase (GiardiaDB identification no. GL50803_16001) and GSH synthase (GiardiaDB identification no. GL50803_15429). Thus, GSH is likely present in *Giardia*, probably at low concentrations which were not detected in the previous study (4).

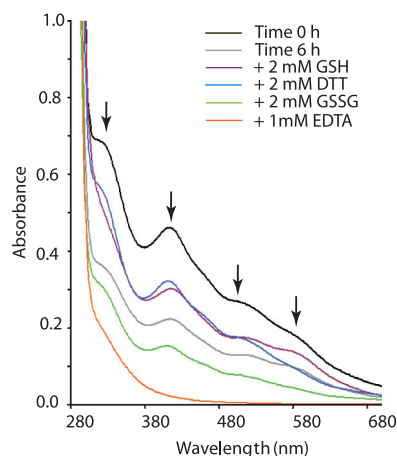


FIG. 7. UV-visible spectrum of recombinant Gigrx indicate presence of FeS cluster. N-terminal truncated Gigrx was produced in *E. coli* and purified to homogeneity. An absorption peak at 410 nm and shoulders at 320, 510, and 590 nm (arrows) were observed, which are characteristic for a [4Fe4S] cluster coordinated by CGFS-type monothiol glutaredoxins. GSSG, GSH disulfide.

Cell localization studies showed that the translocation of Gigrx required an N-terminal extension of 77 amino acids, which is not present in the mature protein immunoprecipitated from *G. intestinalis* mitosomes. The presence of the transcript coding for the complete preprotein including the N-terminal extension was verified by reverse transcription-PCR. No other forms of Gigrx were observed in these mitosomes. The extension is unusually long in comparison to known mitochondrial targeting presequences, which usually comprise 10 to 18 amino acid residues (24). The composition of the Gigrx extension is also unique. While multiple positively charged residues are found within the extension of Gigrx, only a single such residue is found in close proximity to the cleavage site in other mitochondrial proteins. This feature is related to the unique structure of the mitochondrial processing peptidase in *Giardia*, which has evolved toward processing a limited set of substrates (24). Neither mitochondrial nor mitochondrial processing peptidases were able to cleave the Gigrx preprotein in vitro. As a result, the mechanism by which Gigrx is processed upon its translocation to the organelles remains a puzzle.

Recent phylogenetic analysis (16) as well as this report revealed that monothiol CGFS-type Grxs are highly conserved across eukaryotic lineages, being present in organelles of endosymbiotic origin. Interestingly, except for those in *G. intestinalis*, genes coding for CGFS-type Grxs were not found in mitosome-harboring organisms, including *Entamoeba* and *Cryptosporidium* species, and no gene coding for this Grx type was identified in the genome of hydrogenosome-possessing *Trichomonas vaginalis*. A similar glutaredoxin with a CGFT motif was found in the genome of the microsporidium *Encephalitozoon cuniculi* (9). This glutaredoxin was able to restore the growth of *S. cerevisiae* *grx5* mutants when targeted to *S. cerevisiae* mitochondria. However, its cellular localization within *E. cuniculi* cells has not been resolved. In *S. cerevisiae*, the phenotypic defect caused by *grx5* knockout could be suppressed by overexpression of the HSP70-type chaperon Ssq1 and alternative scaffold protein IscA (Isa2) (22). Therefore, the absence of

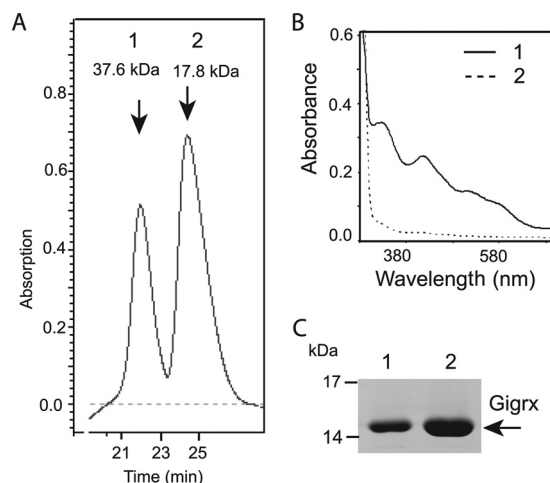


FIG. 8. The FeS cluster is coordinated with homodimeric Gigrx. (A) Gel filtration of recombinant Gigrx showed two protein populations corresponding to dimeric (1) and monomeric (2) structure. (B) Absorption peaks at 320, 410, 510, and 590 nm indicating the presence of an FeS cluster were associated only with the higher-molecular-mass protein (1), while no absorption within this range was obtained with the lower-molecular-mass protein (2). (C) Separation of dimeric Gigrx (1) under denaturing conditions by SDS-PAGE revealed a single protein of identical molecular size to monomeric Gigrx (2).

a CGFS-type glutaredoxin in some mitosomes and hydrogenosomes might be compensated for by these components of the FeS cluster assembly machinery. For example in the *T. vaginalis* genome, there are at least five genes coding for hydrogenosomal HSP70 and four genes for putative IscA, which might be candidates for such a role. In this context two tantalizing questions remain: why was the CGFS-type glutaredoxin retained in the mitosomes of *G. intestinalis*, the proteome of which is highly reduced (24), and what is the exact biochemical role of Gigrx within these enigmatic organelles?

ACKNOWLEDGMENTS

We thank M. Marcinčiková for outstanding technical support and Z. Voburka for amino acid sequencing by Edman degradation.

This work was supported by the Czech Science Foundation (204/06/0947) and by the Ministry of Education of the Czech Republic (MSM0021620858 and LC07032 to J.T.).

REFERENCES

- Adinolfi, S., C. Iannuzzi, F. Prisci, C. Pastore, S. Iametti, S. R. Martin, F. Bonomi, and A. Pastore. 2009. Bacterial frataxin CyaY is the gatekeeper of iron-sulfur cluster formation catalyzed by IscS. *Nat. Struct. Mol. Biol.* **16**: 390–396.
- Alves, R., E. Vilaprinyo, A. Sorribas, and E. Herrero. 2009. Evolution based on domain combinations: the case of glutaredoxins. *BMC Evol. Biol.* **9**:66.
- Bandyopadhyay, S., F. Gama, M. M. Molina-Navarro, J. M. Gualberto, R. Claxton, S. G. Naik, B. H. Huynh, E. Herrero, J. P. Jacquot, M. K. Johnson, and N. Rouhier. 2008. Chloroplast monothiol glutaredoxins as scaffold proteins for the assembly and delivery of [2Fe-2S] clusters. *EMBO J.* **27**:1122–1133.
- Brown, D. M., J. A. Upcroft, and P. Upcroft. 1993. Cysteine is the major low-molecular weight thiol in *Giardia duodenalis*. *Mol. Biochem. Parasitol.* **61**:155–158.
- Dolezal, P., A. Dancis, E. Lesuisse, R. Sutak, I. Hrdy, T. M. Embley, and J. Tachezy. 2007. Frataxin, a conserved mitochondrial protein, in the hydrogenosome of *Trichomonas vaginalis*. *Eukaryot. Cell* **6**:1431–1438.
- Dolezal, P., O. Smid, P. Rada, Z. Zubacova, D. Bursac, R. Sutak, J. Nebesarova, T. Lithgow, and J. Tachezy. 2005. Giardia mitosomes and trichomonad hydrogenosomes share a common mode of protein targeting. *Proc. Natl. Acad. Sci. USA* **102**:10924–10929.

7. Embley, T. M., and W. Martin. 2006. Eukaryotic evolution, changes and challenges. *Nature* **440**:623–630.
8. Feng, Y., N. Zhong, N. Rouhier, T. Hase, M. Kusunoki, J. P. Jacquot, C. Jin, and B. Xia. 2006. Structural insight into poplar glutaredoxin C1 with a bridging iron-sulfur cluster at the active site. *Biochemistry* **45**:7998–8008.
9. Goldberg, A. V., S. Molik, A. D. Tsaousis, K. Neumann, G. Kuhnke, F. Delbac, C. P. Vivares, R. P. Hirt, R. Lill, and T. M. Embley. 2008. Localization and functionality of microsporidian iron-sulphur cluster assembly proteins. *Nature* **452**:624–628.
10. Hall, T. A. 1999. BioEdit: a user-friendly biological sequence alignment editor and analysis program for Windows 95/98/NT. *Nucleic Acids Symp. Ser.* **41**:95–98.
11. Reference deleted.
12. Johnson, D. C., D. R. Dean, A. D. Smith, and M. K. Johnson. 2005. Structure, function, and formation of biological iron-sulfur clusters. *Annu. Rev. Biochem.* **74**:247–281.
13. Keister, D. B. 1983. Axenic culture of *Giardia lamblia* in TYI-S-33 medium supplemented with bile. *Trans. R. Soc. Trop. Med. Hyg.* **77**:487–488.
14. Kispal, G., P. Csere, C. Prohl, and R. Lill. 1999. The mitochondrial proteins Atm1p and Nfs1p are essential for biogenesis of cytosolic Fe/S proteins. *EMBO J.* **18**:3981–3989.
15. Lill, R., and U. Muhlenhoff. 2008. Maturation of iron-sulfur proteins in eukaryotes: mechanisms, connected processes, and diseases. *Annu. Rev. Biochem.* **77**:669–700.
16. Lillig, C. H., C. Berndt, and A. Holmgren. 2008. Glutaredoxin systems. *Biochim. Biophys. Acta* **1780**:1304–1317.
17. Morrison, H. G., A. G. McArthur, F. D. Gillin, S. B. Aley, R. D. Adam, G. J. Olsen, A. A. Best, W. Z. Cande, F. Chen, M. J. Cipriano, B. J. Davids, S. C. Dawson, H. G. Elmendorf, A. B. Hehl, M. E. Holder, S. M. Huse, U. U. Kim, E. Lasek-Nesselquist, G. Manning, A. Nigam, J. E. Nixon, D. Palm, N. E. Passamaneck, A. Prabhu, C. I. Reich, D. S. Reiner, J. Samuelson, S. G. Svard, and M. L. Sogin. 2007. Genomic minimalism in the early diverging intestinal parasite *Giardia lamblia*. *Science* **317**:1921–1926.
18. Muhlenhoff, U., J. Gerber, N. Richhardt, and R. Lill. 2003. Components involved in assembly and dislocation of iron-sulfur clusters on the scaffold protein Isu1p. *EMBO J.* **22**:4815–4825.
19. Muhlenhoff, U., N. Richhardt, J. Gerber, and R. Lill. 2002. Characterization of iron-sulfur protein assembly in isolated mitochondria—a requirement for ATP, NADH, and reduced iron. *J. Biol. Chem.* **277**:29810–29816.
20. Picciocchi, A., C. Saguez, A. Boussac, C. Cassier-Chauvat, and F. Chauvat. 2007. CGFS-type monothiol glutaredoxins from the cyanobacterium *Synechocystis* PCC6803 and other evolutionary distant model organisms possess a glutathione-ligated [2Fe-2S] cluster. *Biochemistry* **46**:15018–15026.
21. Richards, T. A., and M. van der Giezen. 2006. Evolution of the Isd11-IscS complex reveals a single alpha-proteobacterial endosymbiosis for all eukaryotes. *Mol. Biol. Evol.* **23**:1341–1344.
22. Rodriguez-Manzanique, M. T., J. Tamarit, G. Belli, J. Ros, and E. Herrero. 2002. Grx5 is a mitochondrial glutaredoxin required for the activity of iron/sulfur enzymes. *Mol. Biol. Cell* **13**:1109–1121.
23. Ronquist, F., and J. P. Huelsenbeck. 2003. MrBayes 3: Bayesian phylogenetic inference under mixed models. *Bioinformatics* **19**:1572–1574.
24. Smid, O., A. Matuskova, S. R. Harris, T. Kucera, M. Novotny, L. Horvathova, I. Hrdy, E. Kutejova, R. P. Hirt, T. M. Embley, J. Janata, and J. Tachezy. 2008. Reductive evolution of the mitochondrial processing peptidases of the unicellular parasites *Trichomonas vaginalis* and *Giardia intestinalis*. *PLoS Pathog.* **4**:e1000243.
25. Sun, C. H., C. F. Chou, and J. H. Tai. 1998. Stable DNA transfection of the primitive protozoan pathogen *Giardia lamblia*. *Mol. Biochem. Parasitol.* **92**:123–132.
26. Tachezy, J., and P. Dolezal. 2007. Iron-sulfur proteins and iron-sulfur cluster assembly in organisms with hydrogenosomes and mitosomes, p. 105–133. *In* W. Martin and M. Müller (ed.), *Origin of mitochondria and hydrogenosomes*. Springer-Verlag, Berlin, Germany.
27. Tachezy, J., and O. Smid. 2008. Mitosomes in parasitic protists, p. 202–230. *In* J. Tachezy (ed.), *Microbial monographs*. Springer-Verlag, Berlin, Germany.
28. Thompson, J. D., T. J. Gibson, F. Plewniak, F. Jeanmougin, and D. G. Higgins. 1997. The CLUSTAL_X windows interface: flexible strategies for multiple sequence alignment aided by quality analysis tools. *Nucleic Acids Res.* **25**:4876–4882.
29. Tovar, J., G. Leon-Avila, L. B. Sanchez, R. Sutak, J. Tachezy, M. van der Giezen, M. Hernandez, M. Müller, and J. M. Lucocq. 2003. Mitochondrial remnant organelles of *Giardia* function in iron-sulphur protein maturation. *Nature* **426**:172–176.
30. van der Giezen, M. 2009. Hydrogenosomes and mitosomes: conservation and evolution of functions. *J. Eukaryot. Microbiol.* **56**:221–231.
31. Yarunin, A., V. G. Panse, E. Petfalski, C. Dez, D. Tollervey, and E. C. Hurt. 2005. Functional link between ribosome formation and biogenesis of iron-sulfur proteins. *EMBO J.* **24**:580–588.